Title

Buildings Research using Infrared Imaging Radiometers with Laboratory Thermal Chambers

Author

Griffith, Brent

Publication Date

1999-01-12

LBNL-42682

ERNEST ORLANDO LAWRENCE
BERKELEY NATIONAL LABORATORY

Buildings Research Using Infrared Imaging Radiometers with Laboratory Thermal Chambers

Brent T. Griffith and Dariush Arasteh

Environmental Energy Technologies Division

January 1999

Presented at
Thermosense XXI,
Orlando, FL,
April 5–9, 1999,
and to be published in
the Proceedings

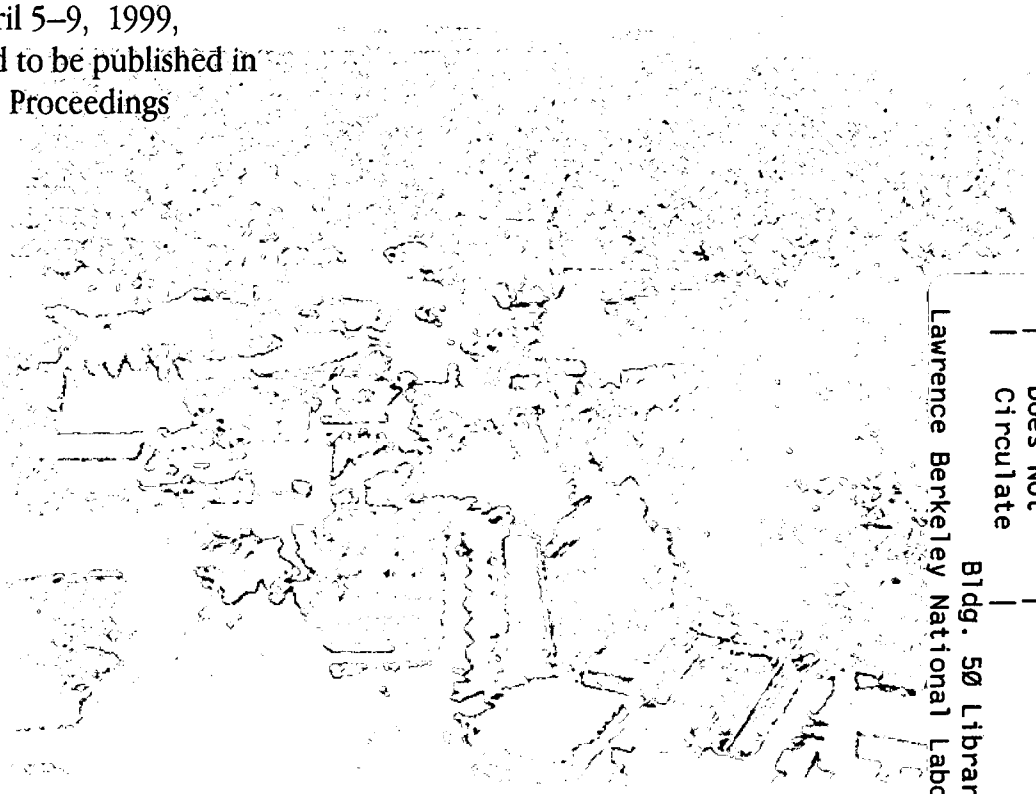

DISCLAIMER

LBNL-42682
TA-398

Proceedings of the SPIE, Vol. 3700, April 6-8, 1999.

Buildings Research Using Infrared Imaging Radiometers with Laboratory Thermal Chambers

Brent T. Griffith and Dariush Arasteh

Windows and Daylighting Group
Building Technologies Department
Environmental Energy Technologies Division
Ernest Orlando Lawrence Berkeley National Laboratory
University of California
1 Cyclotron Road
Berkeley, CA 94720

January 1999

This work was supported by the Assistant Secretary for Energy Efficiency and Renewable Energy, Office of Building Technology, State and Community Programs, Office of Building Systems of the U.S. Department of Energy under Contract No. DE-AC03-76SF00098.

Buildings Research Using Infrared Imaging Radiometers with Laboratory Thermal Chambers

Brent T. Griffith and Dariush Arasteh
Building Technologies Department
Environmental Energy Technologies Division
Ernest Orlando Lawrence Berkeley National Laboratory

ABSTRACT

Infrared thermal imagers are used at Lawrence Berkeley National Laboratory to study heat transfer through components of building thermal envelopes. Two thermal chambers maintain steady-state heat flow through test specimens under environmental conditions for winter heating design. Infrared thermography is used to map surface temperatures on the specimens' warm side. Features of the quantitative thermography process include use of external reference emitters, complex background corrections, and spatial location markers. Typical uncertainties in the data are +/- 0.5°C and 3 mm. Temperature controlled and directly measured external reference emitters are used to correct data from each thermal image. Complex background corrections use arrays of values for background thermal radiation in calculating temperatures of self-viewing surfaces. Temperature results are used to validate computer programs that predict heat flow including Finite-Element Analysis (FEA) conduction simulations and conjugate Computational Fluid Dynamics (CFD) simulations. Results are also used to study natural convection surface heat transfer. Example data show the distribution of temperatures down the center line of an insulated window.

INTRODUCTION

Building scientists are interested in thoroughly understanding the thermal performance of buildings' exterior shells, which form the barrier between the outdoor weather and conditioned inside space. A building's thermal envelope consists of the outer walls, windows, and roof and other places where insulated building components are located in order to increase the efficiency of building heating and cooling. Heat flow through the building thermal envelope is assessed in detail in order to (1) predict thermal loads for the design of heating and cooling systems, (2) investigate methods to improve control of heat losses/gains, (3) predict how the built environment will affect occupant thermal comfort, and (4) allow for fair comparisons between competing products and designs. For example, it is useful to quantify the difference between the thermal resistance of a wall system with steel framing members and with wood studs, or to be able to accurately judge the energy impacts of two different window products.

The Infrared Thermography Laboratory (IRLab) was established at Lawrence Berkeley National Laboratory (LBNL) to use infrared imaging radiometers (IR imagers) to produce detailed maps of the surface temperature of building specimens while heat is flowing through them. Test specimens are mounted between two temperature-controlled environmental chambers in a fashion similar to that used for hot-box testing for measuring the U-Factor (or R-Value) of wall systems and window products. These more conventional tests determine the spatially averaged heat flux (per unit area, per unit temperature difference) for measured specimens. In contrast, the IRLab tests determine spatial distributions of surface temperatures and therefore provide considerably more information on localized thermal phenomena. Using IR imagers to perform quantitative thermography provides experimental results that allow analysis of two- and three-dimensional heat flows, thermal bridges, and natural convection.

This paper summarizes the techniques currently used in the IRLab to perform quantitative infrared thermography and explains how the results are used to validate computer simulations of steady state heat flow. We first discuss the thermal chambers used to drive heat flow through building specimens and then describe how test specimens are prepared. Much of the paper focuses on the distinctive features of the experimental procedures and data processing techniques used to perform quantitative thermography for

these thermal tests. Example data are shown for test specimens designed to evaluate thermally insulated windows.

LABORATORY THERMAL CHAMBERS

Because the building assemblies evaluated in the IRLab are passive components with no internal heat sources or sinks, two environmental chambers with different air temperatures-a climate chamber and a thermography chamber-are used to generate steady-state heat flow across test specimens. One chamber is referred to as the thermography chamber because infrared thermographic measurements take place here. This chamber is usually controlled to provide stable room temperature with nominally still air. The other chamber is referred to as the climate chamber because it simulates cold weather on the outside surface of a building component during the heating season. The test conditions are chosen to match the design conditions recommended by the American Society of Heating Refrigerating and Air-Conditioning Engineers (ASHRAE) for determining thermal loads in sizing mechanical equipment. ASHRAE winter design conditions specify cold-side conditions of –17.8°C with a mean surface heat transfer coefficient of 29 W/m^2-K and warm-side conditions of 21.1°C and 7.9 W/m^2-K. The thermal chambers used in the IRLab are discussed below and diagrammed in Figure 1.

Climate Chamber

The climate chamber used at the IRLab, see Figure 1, is a modified commercial food freezer. Air flow is upwards and parallel to the test specimen, with a plenum (baffle) depth of 10 cm from the specimen surface. The entire air flow is routed through ducts that have nearly constant cross-section size and rounded corners where the wind changes direction. Air leaving the blower circulates upward across the specimen, is forced through the cooling coil, passes strip heaters, and then returns to the blower. The air blower is a custom-made, constant-speed, axial cross-flow fan with a diameter of 10 cm. The fan width is more than 95% of the entire plenum width. This design insures a uniform air velocity profile across the width of the air flow plenum and efficient use of cooling power. Absolute air speed ranges between 3.9 and 6.0 m/s, depending on chamber operation and specimen geometry. A horizontal array of three separately controlled electrical strip heaters is installed between the cooling coil and the blower. Three separate zones (across the width if the plenum) are controlled with instruments capable of ±0.05°C accuracy. The overall surface conductance has been measured at 30 ±5 W/m^2·K. Because of the high surface conductance, the temperature difference between air and the specimen surface is typically 1° to 4°C, depending on specimen properties and geometry, and the radiation heat transfer to the plenum is low.

Thermography Chamber

The thermography chamber allows for control and measurement of air temperature and velocity on one face of a specimen under uniform thermal radiation conditions and for an IR imager to measure the specimen. The thermography chamber used at the IRLab has an outer size of 1.4 m wide and 2.1 m high with a depth that can vary from 0.9 to 4.2 m (see Figure 1). It is a sandwich construction of sealed plywood and extruded polystyrene foam boards. Extendible bellows allow for an airtight variable viewing distance. The IR imager may be located outside the chamber using an airtight view port or the scanner head may be mounted inside the chamber and operated remotely. Air circulation and conditioning equipment is located in a subfloor beneath the specimen and viewing enclosure. A 50-mm slot runs across the entire width of the subfloor at the edge beneath the specimen creating an air sink that drains cooler air running off the specimen into the subfloor. At the opposite edge of the subfloor, a 40-mm-wide output slot introduces conditioned air at low velocity to the warm chamber. A recirculating air mixing chamber within the subfloor has much higher air velocities to improve heat exchange with the cooling coil and heaters. Five variable-speed fans force air through a custom-built heat exchanger cooled with temperature-controlled recirculating fluid. The slightly chilled air is then reheated by three individually controlled, flat-sheet heaters. A partition is used to recirculate most of the air back to the fan intake, bypassing the main chamber. The fan-induced pressure differences between the intake and output

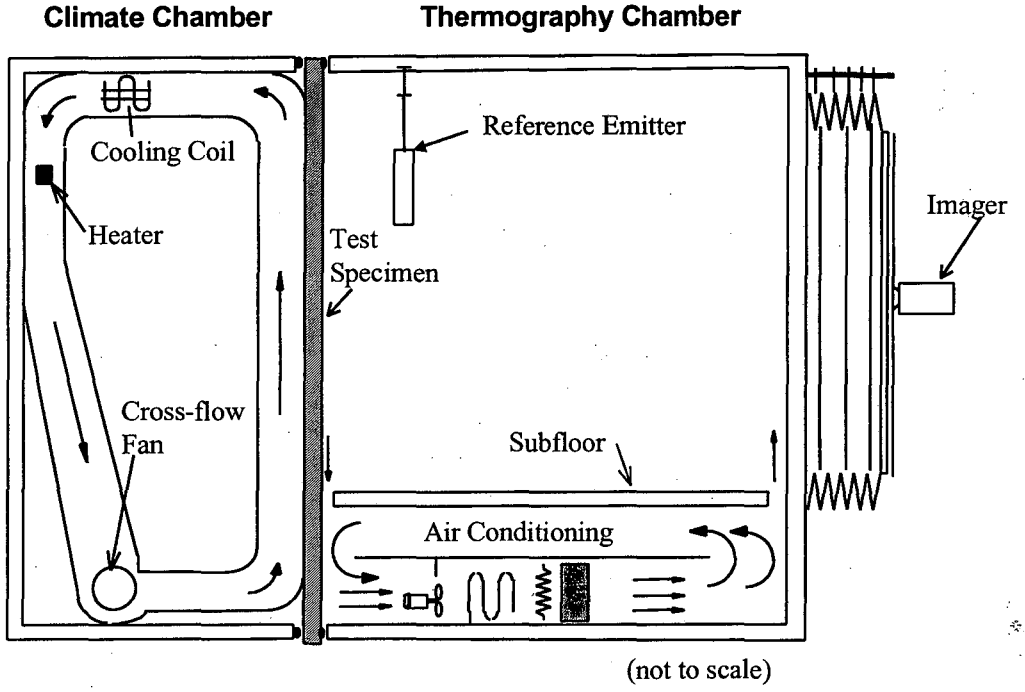

Figure 1. Laboratory Thermal Chambers Used to Generate Steady-State Heat Flow through Building Specimens

slots cause a small volume of air to be exchanged with the warm chamber. The overall surface conductance has been measured from 7 to 9.5W/m²·K, depending on fan power settings, but is usually close to 8.0 W/m²·K. The temperature difference between enclosure surfaces and the specimen is usually 3° to 15°C. Thermal radiation is about half of the total surface conductance at the specimen. An attached air dryer is used to lower humidity levels so that condensation on cold specimen surfaces can be avoided. The chamber is also equipped with a computer-controlled traversing system for remote and programmable motion of the imager and/or other sensors.

TEST SPECIMENS

The test specimens are prepared and mounted in a foam panel that surrounds them, and then situated between the two thermal chambers. Unless the effects of air leakage through the specimen are being evaluated, the specimens are sealed with adhesive tape and/or silicone sealant so that air is not able to exchange between the two chambers. If a specimen has an emittance below 0.5 it is coated with water-based temporary paint or paper adhesive tape. The specimen is then placed into a close-fitting foam panel and sealed on both sides to prevent any leaks around the specimen periphery. The insulated surrounding panel holds the specimen in place and separates the cold chamber from the warm chamber. Markers are applied to the specimen surface so that locations can be determined in the thermographic images. The markers are strips of aluminum tape, 3 by 50 mm, used in pairs to mark the endpoints of lines that will be used to locate the regions of the specimen being measured. (Figure 7 shows some location markers.)

Research in the IRLab has focused on fenestration specimens such as insulated glazing units and windows. Wall and roof systems could be tested in a similar fashion, but windows have received more attention because of national efforts to rate and label their thermal performance and because of the authors' interests in researching efficient window technologies. Testing has focused on three kinds of fenestration specimens: (1) complete insulated window products, (2) insulated glazing units, and

(3) calibrated transfer standards. Insulated glazing units are sealed assemblies of two (or more) separated glass sheets that are installed in a window frame to make a complete insulated window product. A Calibrated Transfer Standards (CTS) is a special test specimen used in standardized thermal testing of window products to characterize surface heat-transfer conditions for the thermal chambers being used in the test[1]. A CTS has two sheets of glass separated by foam board and is instrumented with temperature sensors.

This paper presents the distribution of temperatures on the lower edge of the CTS and along the centerline of a dual-pane insulated glazing unit. The CTS has been selected as an example because it is a relatively simple test specimen with the advantage of embedded temperature sensors that provide an independent means of determining surface temperature, which permit us to verify results based on infrared (see Figure 2). Because the CTS is mounted so that it is recessed into the surrounding foam panel it also shows the complexity involved in imaging specimens with self viewing surfaces as well as combining data from different viewing angles. The two sheets of glass in the CTS are separated by a 12.6 mm thick foam board. The double pane insulated glazing unit was selected as an example because two independent laboratories produced experimental results for the same specimen, and two other researchers produced simulation results in a collaborative project (see Figure 3); we show how results from several sources can be compared. The two sheets of glass are sealed around the perimeter with an insulating foam spacer system that forms a 12.5 mm air gap.

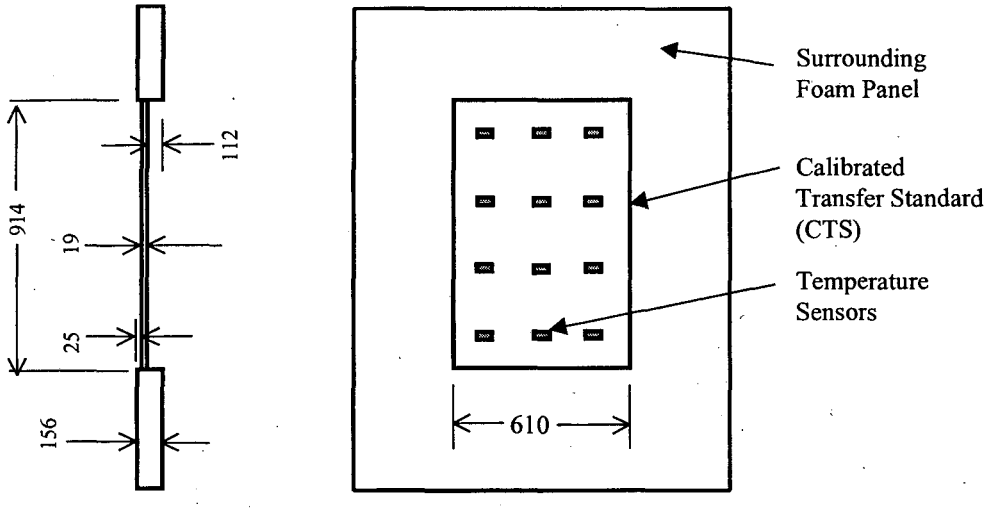

Figure 2. CTS Test Specimen and Mounting

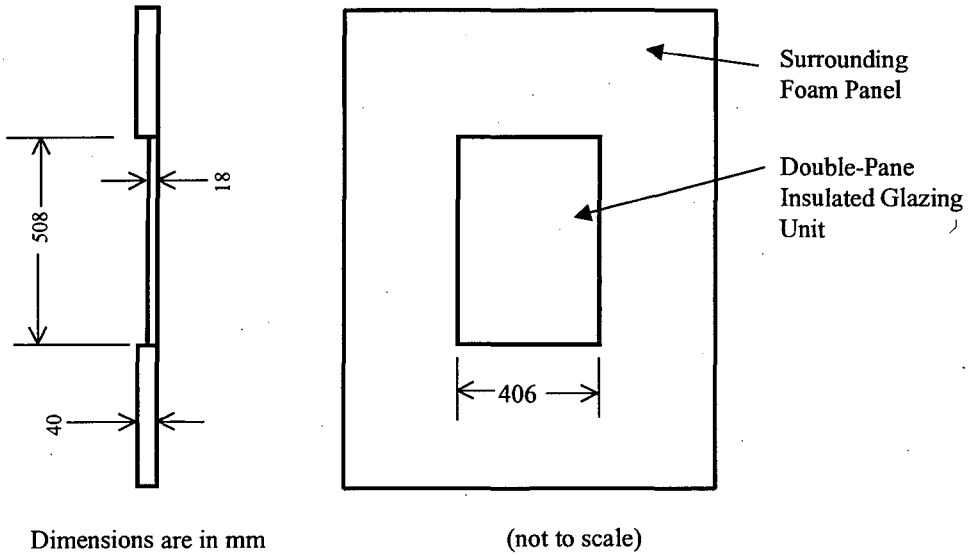

Figure 3 Insulated Glazing Unit Test Specimen and Mounting

QUANTITATIVE THERMOGRAPHY

Building scientists can effectively use infrared measurements of surface temperature if the accuracy of these measurements is better than typical equipment specifications (2% or 2°C). There may, for example, be only a 1°C difference between ambient room air temperature and the surface temperature of a highly insulated specimen. Therefore, measurement uncertainty less than 1°C for absolute temperature is desirable. To obtain this level of accuracy using infrared imagers requires careful procedures and data processing. The section below summarizes the techniques used in our laboratory to achieve uncertainties of about ± 0.5°C for typical measurements.

Measurement Procedures

The overall design of our thermal tests facilitates accurate infrared temperature measurements. The measurements are conducted in a special chamber designed to provide stable thermal conditions with uniform surface temperatures. Because heat flow is steady-state and controlled, we can improve the accuracy and resolution of measurements by: averaging measurements over time, repeating measurements, using multiple views, and positioning background mirrors. This paper does not thoroughly describe procedures for operating an infrared imager and collecting thermographic data; we focus instead on three procedural details that are important for quantitative thermography: (1) determining emittance, (2) scaling with an external reference emitter, and (3) measuring background levels at each data point. Emittance values should be accurate and not adjusted so that infrared results match a known temperature. Including an external reference emitter in each image provides an effective means for calibrating the thermographic data. Collecting arrays of values for the background radiation level allows us to account for reflected radiation at self-viewing surfaces.

Emittance

Emittance describes the ability of a body to emit radiation. We need to figure out the appropriate emittance value for the particular material in each specimen and for the IR imager being used. Emittance is defined as the ratio of the rate of radiant emission of the body, as a consequence of temperature only, to

the corresponding emission of a perfect emitter (blackbody) at the same temperature. Although this term refers to a basic material property that in principal has one true value, it is used here in a slightly different fashion: the appropriate emittance value to use for quantitative infrared thermography is scaled by the wavelength-dependent response of the detector used in the radiometer. This emittance value may differ from literature values and may vary among different radiometers. Thus in our procedures, the appropriate values to use for emittance of the various materials on a specimen's surface are first measured in a separate experiment that compares the specimen's emittance to the emittance of known material. Thin specimens of both a known material and the unknown sample material are mounted in good thermal contact to an isothermal, temperature-controlled plate and brought to the same surface temperature. The temperature is set approximately 10° to 20°C above or below the background temperature to insure high contrast between the radiosity from the specimens and the radiation from the background. The infrared imager is set to emittance 1.0 to turn off any background radiation compensation. Both specimens are imaged simultaneously. Readings are averaged over both time and space for the equivalent blackbody temperature of the unknown sample, $\mathbf{T_{e=1,smpl}}$, and the equivalent blackbody temperature of the known reference material, $\mathbf{T_{e=1,ref}}$. Background radiation equivalent blackbody temperature, $\mathbf{T_{back}}$, is quantified using a background mirror. Caution is exercised to provide a very uniform background, which is verified by imaging the background mirror. The emittance of the sample material, $\mathbf{e_{smpl}}$, is then calculated from the emittance of the known material, $\mathbf{e_{ref}}$, using equation 1. Temperature units are Kelvin. Several measurements are made and then averaged.

$$e_{smpl} = \frac{\left(T^4_{e=1,smpl} - T^4_{back}\right)}{\left(T^4_{e=1,ref} - T^4_{back}\right)} e_{ref} \qquad (1)$$

For example, using this procedure we determined that the best value to use is 0.86 for soda-lime float glass commonly used in windows. This is in contrast to the typical literature value of 0.84 for total hemispherical infrared emittance for all infrared wavelengths. If the spectral data for emittance are weighted uniformly over just the wavelength range of our detector (8 to 12 microns), then the literature data for glass produce an emittance value of 0.87. This discrepancy shows the importance of conducting an ancillary experiment in order to determine the most accurate emittance value to use for each material and detector.

External Reference Emitter

An external reference emitter is used to increase the accuracy of thermographic measurements[2]. A reference emitter is a temperature-controlled device with a known surface emittance. During each measurement, the reference emitter is situated near the specimen being measured and within the field of view of the IR imager. The reference emitter is kept reasonably in focus while the imager is focused on the test specimen. The temperature of the reference emitter as measured with infrared is compared to direct contact measurements, and deviations are used to scale the infrared results for the test specimen.

Although a commercially available extended-area blackbody (of the type used to calibrate IR imagers) has been used in the past, the reference emitter used most often in the IRLab is a custom device based on a temperature-controlled liquid system (shown in Figure 4). One continuous fluid channel made of two concentric rectangular spirals with opposing directions was machined out of a solid block of copper, leaving a 13-mm-thick solid portion directly underneath the reference surface. This design minimizes temperature gradients across the surface because heat is continuously exchanged between the liquid supply and return inside the block. A bore reaches to the center of the solid portion that accommodates a laboratory-grade, platinum resistance temperature (PRT) probe with a system accuracy of ±0.02°C. Enough copper surrounds the bore that no discernible temperature gradients occur on the reference emitter surface. The backs of the fluid channels in the block are sealed with an additional copper plate.

Except for the reference surface, the entire device and the liquid supply and return lines are insulated. A thin sample of the same material as the test specimen is mounted on the reference emitter using a heat sink compound. The temperature-controlled liquid is supplied by a recirculating bath with a built-in microprocessor controller. The reference emitter is designed and placed so that its presence interferes minimally with air temperature and flow results. The reference emitter surface temperature is adjusted from substrate measurements to account for heat flow and temperature gradients through the surface material and determined with an absolute accuracy of ± 0.1°C.

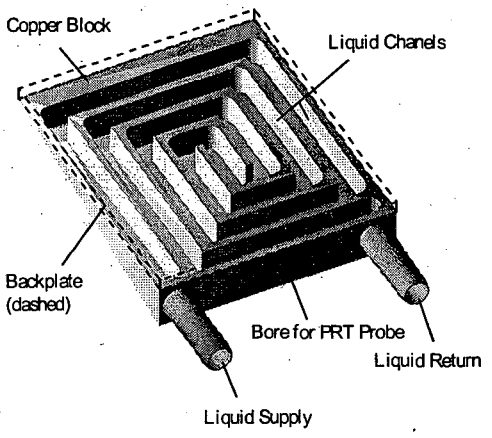

Figure 4. Copper Block Inside the Custom-Built Reference Emitter

Complex Background Radiation

Because real materials are not perfect emitters, some portion of the radiation emanating from a surface is reflected. In order to calculate a temperature result, we quantify the level of background radiation arriving at the surface (irradiance) by using an equivalent blackbody temperature, $\mathbf{T_{back}}$. When infrared measurements are limited to flat, flush-mounted specimens, there is no way for the different parts of the specimen surface to directly exchange thermal radiation. In this case, $\mathbf{T_{back}}$ will be determined by the temperature of the enclosure surfaces, and a single value can reasonably be used for the entire surface. However, when a specimen has self-viewing surfaces, as shown in Figure 5, the background radiation level for certain measurements is affected by the other portions of the specimen and not necessarily the enclosure surfaces. If the reflections are specular, the background radiation involved in an infrared temperature measurement of point **A** in Figure 5 will originate from point **B**. Point **B** is on the specimen. Thus, the background radiation level for point **A** depends on the temperature at point **B,** which will differ from the enclosure surface temperature. We refer to the technique for measuring self-viewing surfaces as complex background thermography.

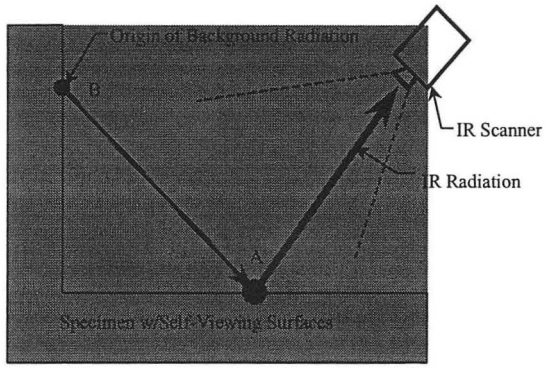

Figure 5. Complex Background Thermography

In contrast to IR thermography for flat surfaces, complex background thermography requires additional steps to gather background radiation levels. The values for $\mathbf{T_{back}}$ are measured by applying background mirrors (aluminized polyester film) to the specimen in at least two stages. Mirrors are applied directly to specimen surfaces, so the background radiation can be measured for that particular surface. For the setup in Figure 5, a mirror would be applied to surface **A** after the specimen has been measured. Then, after the mirror reflections at surface **A** are captured as a thermogram, the mirror would be removed and a new mirror applied to surface B. Thermal equilibrium would be established between each step, and the scanner viewing angle and specimen geometry would remain the same. If a specimen such as a window frame has numerous planes with different orientations, then each plane needs to be mirrored in a separate step so that background mirrors do not view other background mirrors. Mirror size is kept relatively small in order to lessen the effect of reduced surface emissivity on the overall thermal situation.

Data Processing

Because measurements in the IRLab are part of a meticulous case-by-case research effort rather than a routine testing program, considerable time and effort can be put into processing raw data and producing the most accurate results. In order to obtain quantitative surface temperatures, the raw thermographic data are first extracted from the thermography software so they can be processed in a mathematical program. Usually the effort focuses on obtaining results along just the center line of the test specimen for use in validating computer programs that simulate two-dimensional cross sections. Data are extracted from the thermogram as appropriate arrays of text values and synchronized with spatial coordinates. The result for temperature at each data point is calculated with the correct emittance and a location-specific background level. The calculated infrared temperature for the reference emitter is compared to direct contact measurements, and deviations are used to scale the rest of the infrared data. Several data sets are sometimes merged together to combine data from different close-up views.

Numerical text data are extracted from the thermographic image to obtain arrays of values for subsequent processing. Figure 7 shows a thermographic image of the sill of the CTS specimen. Overlay boxes are draw on the thermographic image with the help of the location markers. Figure 7 shows the overlay boxes for three different surfaces on the specimen as well two for the reference emitter. The numerical data are then exported from the thermography software. Because we want to obtain data along the vertical center line, the data are averaged across the width of the overlay boxes.

Equation 2 shows an expression for calculating a surface temperature, $\mathbf{T_{IR}}$, from the total thermal radiation represented by the variable $\mathbf{T_{e=1}}$, the emittance of the surface, $\mathbf{e_{surf}}$, and the background radiation level represented by the variable $\mathbf{T_{back}}$. $\mathbf{T_{e=1}}$ is an equivalent blackbody temperature for the surface being

measured. $\mathbf{T_{back}}$ is the equivalent blackbody temperature for the background thermal radiation level as measured at each location with the aid of an applied mirror. Values for both $\mathbf{T_{e=1}}$ and $\mathbf{T_{back}}$ are obtained from the thermography system by setting emissivity to unity.

$$T_{IR} = \left(\frac{(T_{e=1}^4 - (1 - e_{surf}) T_{back}^4)}{e_{surf}} \right)^{1/4} \tag{2}$$

Equation 2 is used to determine both the apparent reference emitter temperature, $\mathbf{T_{IR,Ref}}$, (as measured by infrared) and the apparent sample surface temperature, $\mathbf{T_{IR,smpl}}$. The difference between $\mathbf{T_{IR,Ref}}$ and the direct contact measured value, $\mathbf{T_{DC,Ref}}$, is then applied to correct $\mathbf{T_{IR,smpl}}$ and to arrive at the final surface temperature result, $\mathbf{T}$, as shown in equation 3. This correction is carried out for each temperature datum and for each thermogram to produce arrays of temperature values.

$$T = T_{IR,smpl} - (T_{IR,Ref} - T_{DC,Ref}) \tag{3}$$

Final data sets merge spatial location coordinates with temperature values. The real distances between location markers on the specimen are measured, and a coordinate system is used to create temperature/location data pairs. The temperatures are distributed linearly. Temperature data is then made into a function of x and y spatial coordinates, mapped to the coordinate system being used. The data sets usually have the form (T, x, y). But it is common to present data in the form (T, d), where d is the accumulated distance along the surface, because this is easier to plot.

Quantitative thermography requires a careful estimate of uncertainty in the data. A previous publication by the authors discusses in detail the origination of the following equations used to propagate uncertainty[3]. Errors in $\mathbf{e_{surf}}$ should be treated as a source of nondefinable systematic uncertainty, $\delta\mathbf{e_{surf}}$, and may be analyzed by propagating uncertainty in equation 1. Errors in $\mathbf{T_{e=1}}$ and $\mathbf{T_{back}}$ lead to random uncertainties, $\delta\mathbf{T_{e=1}}$ and $\delta\mathbf{T_{back}}$. $\delta\mathbf{T_{e=1}}$ and $\delta\mathbf{T_{back}}$ are usually closely related to equipment specification for Noise Equivalent Temperature Difference (NETD). To analyze error propagation in equation 2 we calculate the sum of the squares of partial differentials of equation 2 with respect to variables $T_{e=1}$, T_{back}, and e_{surf}, which leads to one possible solution, shown in equation 4. The uncertainty in T_{IR}, $\delta\mathbf{T_{IR}}$, is then calculated using equation 4.

$$\delta T_{IR} = \frac{1}{4}\left(\frac{T_{e=1}^4}{e_{surf}} + T_{back}^4 - \frac{T_{back}^4}{e_{surf}} \right)^{\frac{3}{4}} \left(\sqrt{ \left(4\frac{\delta T_{e=1}}{e_{surf}} T_{e=1}^3 \right)^2 + \left(4T_{back}^3 \delta T_{back} - 4\frac{\delta T_{back}}{e_{surf}} T_{back}^3 \right)^2 + \left(\frac{\delta e_{surf}}{e_{surf}^2} T_{back}^4 - \frac{\delta e_{surf}}{e_{surf}^2} T_{e=1}^4 \right)^2 } \right) \tag{4}$$

The total uncertainty in the final surface temperature, $\delta\mathbf{T}$, is obtained with equation 5. Values for both $\delta\mathbf{T_{IR,smpl}}$ and $\delta\mathbf{T_{IR,Ref}}$ are obtained using equation 4. The uncertainty in the direct contact measurement of the reference emitter surface temperature, $\delta\mathbf{T_{DC,Ref}}$, is determined from the system accuracy of the direct contact sensor combined with any errors associated with adjustments that correct for gradients in the surface material. The uncertainty arising from variations across the field of view, $\delta\mathbf{T_{FOV}}$, is determined from the magnitude of deviations in heavily averaged data for an isothermal plate that fills the section of the field of view being used.

$$\delta T = \delta T_{IR,smpl} + \delta T_{IR,Ref} + \delta T_{DC,Ref} + \delta T_{FOV} \tag{5}$$

RESULTS

The temperature distribution along the lower portion of the CTS is interesting because this region experiences the coldest temperatures (and is therefore the region that performs most poorly from a

building thermal envelope standpoint and is the first place where condensation forms). The viewing arrangements diagrammed in Figure 6 show the self-viewing surfaces-the glass pane and the sill-in this bottom region of the CTS test specimen. Figure 6 also shows the two imager views used to measure the specimen with a close-up, 45° angle shot for the sill corner and with a longer straight-on shot for the entire lower half of the CTS. Figure 7 shows the raw thermographic image from the close-up view of the sill corner region with the reference emitter on the right. Figure 8 shows the exact same close-up view but with background mirrors placed on the vertical surfaces along the region being measured. The results for temperature along this lower half of the CTS specimen are shown in Figure 9. The x axis is accumulated distance from the lower edge of the CTS glass so negative numbers are on the surrounding foam panel and positive numbers extend up the glass. Data up to 100 mm was from the close-up view and data from 100 to 400 mm was from the straight-on view. The values measured for background radiation are shown in Figure 9. Results from the CTS's embedded thermocouples are also provided for the two available locations. In order to show how these results are used in building science, the thermal test of the CTS was also simulated using a two-dimensional FEA program[4] and results plotted in Figure 9. These simulations used ASHRAE design conditions for the boundary conditions on the cold side, but on the warm side radiation was modeled directly using view factor analysis along with a convection coefficient of 3.3 W/m^2-K.

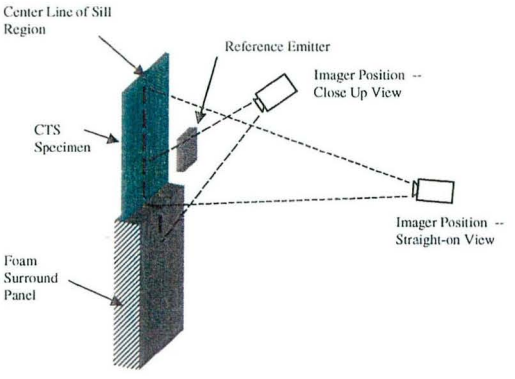

Figure 6. View Arrangements for CTS Measurements

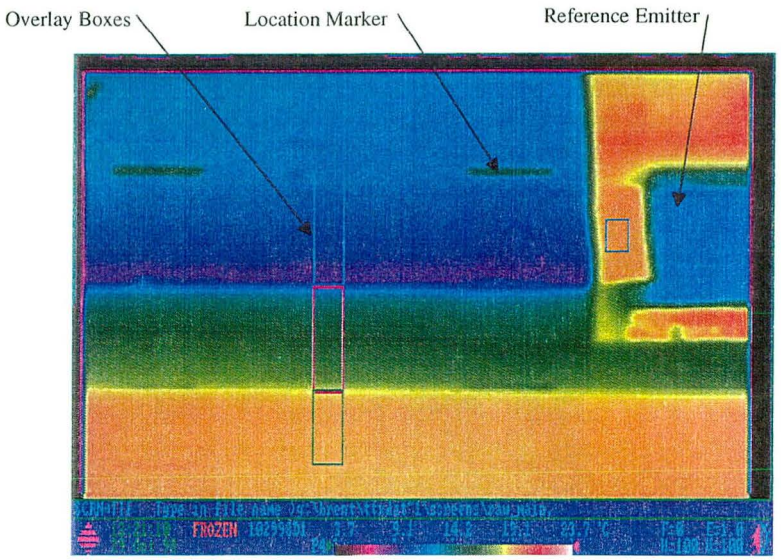

Figure 7. IR Image from Close-Up View of CTS Sill Region

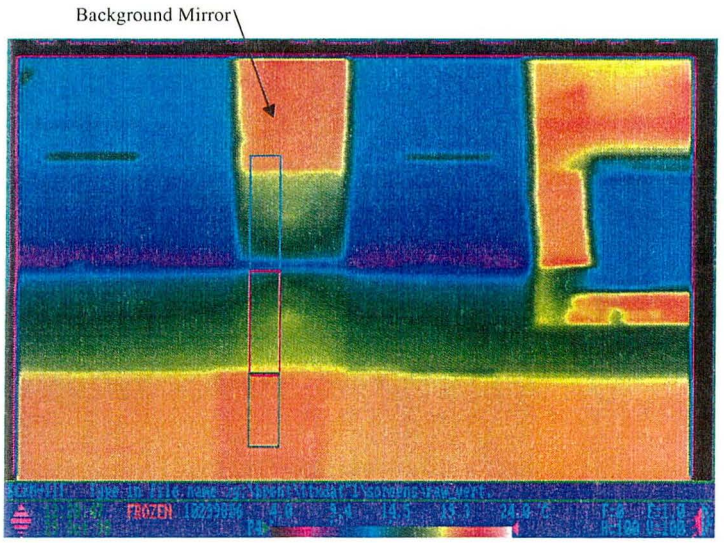

Figure 8. IR Image from Close-Up View of CTS with Background Mirrors on Vertical Surfaces.

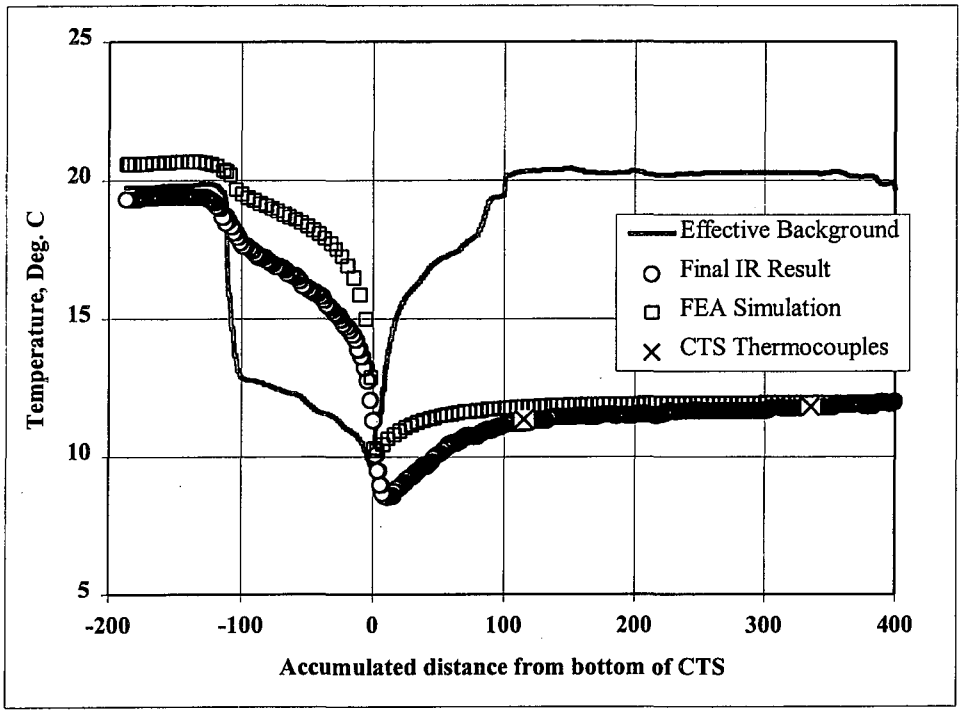

Figure 9. Temperature Profile along Sill of the CTS with Interim Data Used to Determine Final Result

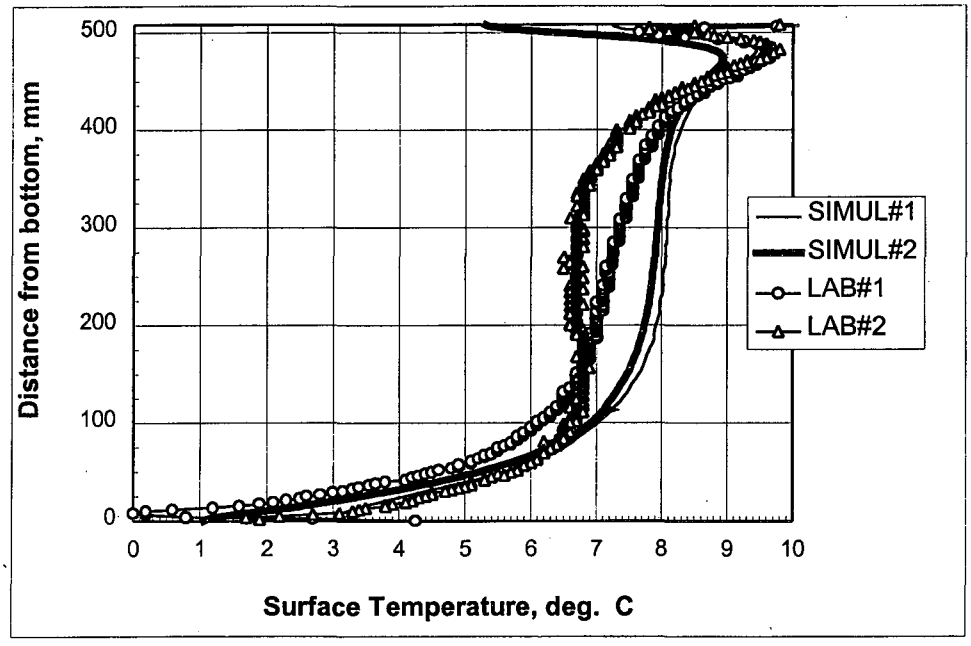

Figure 10. Temperature Profiles along a Dual-Pane Insulated Glazing Unit: Data from Two Laboratories and Two Simulators

Figure 10 shows the results for one of the specimens from a collaborative research project that studied the same set of insulated glazing units[5]. The project focused on comparing results for the vertical distribution of surface temperatures down the center lines of insulated glazing units. Two laboratories measured

specimens using infrared thermography[6,7]. Two separate groups simulated heat flow using conjugate Computational Fluid Dynamics modeling tools

A typical analysis of error using real values from infrared temperature measurements conducted at the IRLab is provided as an example and to show that the estimated uncertainties are within ±0.5°C. This example is for a thermogram that was recorded using an average of 50 frames over time. The specimen and the reference emitter both have normal window glass as the surface material with $e_{surf} = 0.86$ and $\delta e_{surf} = \pm 0.01$. Values of $\delta T_{e=1}$ and δT_{back} are both ±0.05 from the NETD specification of the imager. Other inputs for equation 4 include $T_{e=1} = 291.2K$ and $T_{back} = 294.3K$. Equation 4 then returns $\delta T_{IR} = \pm 0.072°C$. This uncertainty applies to infrared measurements of both the sample and the reference emitter, so $\delta T_{IR,smpl} = \delta T_{IR,Ref} = \pm 0.072°C$. Uncertainty arising from performance variations across the field of view is estimated at $\delta T_{FOV} = \pm 0.2°C$. Uncertainty in the direct contact measurement of the reference emitter surface is estimated at $\delta T_{DC,Ref} = \pm 0.15°C$. Combining uncertainty using equation 5 yields a total estimate for uncertainty in the final temperature of $\delta T = \pm 0.5°C$.

DISCUSSION

The procedures used in the IRLab improve the accuracy of quantitative thermography. While additional effort is required during both imaging and post processing, the resulting data are more accurate and therefore more useful to building scientists during efforts to validate simulations. Developing techniques for measuring self-viewing surfaces has helped expand the number of kinds of specimens that can be tested. The custom-built, fluid-based reference emitter was found to be more useful than air-based, extended-area-blackbodies because it disrupts the experiment less; using the same material on the reference emitter that is on the specimen also reduces (but does not remove) errors associated with correcting for emittance and background radiation. Location markers are a practical method for identifying spatial features in the image so that spatial coordinates can be assigned to the temperature results. Thermal test chambers are effective for such testing when they are specially designed for thermography.

The CTS results shown in Figure 9 are a good example of quantitative thermography. That fact that data from two separate images align well enough to form a smooth temperature curve at 100 mm shows that the data are internally consistent. The data from direct contact measurements using thermocouples agree with the infrared data to within ±0.1°C showing that the infrared measurements have good absolute accuracy (estimated uncertainty in the IR data is ±0.5°C). We also see that the spatial resolution of the infrared data is higher than the resolution of the FEA mesh indicating that such experimental data are well suited for validating computer simulations. The data for $\mathbf{T_{back}}$ vary by as much as 10°C from one location to another and were found to be lower than the measured surface temperature in some cases. This shows that collecting arrays of effective background temperature will produce substantially different (and more accurate) measurements than using a single value for $\mathbf{T_{back}}$ for the entire thermogram.

The results from the simulations and the experimental measurements compare reasonably well although there are some deviations. The temperature curves show the same overall shape and features indicating that the models are fairly good at capturing most of the heat flow phenomena including corner effects (bottom edge of CTS in Figure 9) and thermal bridging (glazing spacers at the top and bottom of Figure 10). Both Figure 9 and Figure 10 show deviations in surface temperature results that indicate simulations over-predict the local temperatures on lower sections of the model. In reality, the natural convection situation at the warm side surface is complicated and the computer models are not able to capture all the subtle details of buoyancy driven air-flow. The simulations of the insulated glazing unit (Figure 10) used CFD methods to model the gas cavity inside the glazing but they used constant film coefficients along the warm-side surface. Thus we can see that the model of the glazing cavity inside the specimen performs well and to further improve the model, simulators should address the localized convection on the outer

surface facing the warm side. In this way, accurate thermographic data allows analyzing the details of natural convection. The temperature data are fairly straightforward to obtain compared to air velocity and are therefore well suited to validate conjugate CFD simulations. The advancement in computer simulation capabilities afforded by such experimental data will lead to more accurate predictions of local surface temperature of components in the building thermal envelope.

CONCLUSIONS

The procedures used in the IRLab at LBNL and analysis of results from studies performed there lead to the following conclusions and observations:

1. Quantitative infrared thermography can provide useful surface temperature data for evaluating the performance of building thermal envelope components. The detailed localized data that are obtained augment measurements of average thermal transmittance.
2. Reference emitter techniques are useful for improving the absolute accuracy of temperature values measured using infrared.
3. Measuring and calculating with arrays of background temperature values improves the accuracy of infrared measurements of specimens that have self-viewing surfaces.
4. Thermography is well suited for investigating *localized* surface conductance phenomena and for comparing to computer simulation results for model validation.

ACKNOWLEDGEMENT

The authors thank Nan Wishner for her assistance in editing this paper. This work was supported by the Assistant Secretary for Energy Efficiency and Renewable Energy, Office of Building Technology, State and Community Programs, Office of Building Systems of the U.S. Department of Energy under Contract No. DE-AC03-76SF00098.

REFERENCES

1. ASTM C 1199, "Standard Test Method for Measuring the Steady-State Thermal Transmittance of Fenestration Systems Using Hot Box Methods." 1995 Annual Book of ASTM Standards, vol. 04.06, pp. 658-669, 1995.
2. B.T. Griffith, F. Beck, D. Arasteh, and D. Türler, "Issues associated with the use of infrared thermography for experimental testing of insulated systems." *Proceedings of the Thermal Performance of the Exterior Envelopes of Buildings VI Conference.* American Society of Heating, Refrigerating and Air-Conditioning Engineers, Atlanta GA, 1995.
3. D. Türler, B.T. Griffith, and D. Arasteh, "Laboratory Procedures for Using Infrared Thermography to Validate Heat Transfer Models." *Insulation Materials: Testing and Applications: Third Volume,* ASTM STP 1320, R. S. Graves and R. R. Zarr, Eds., American Society for Testing and Materials, 1997.
4. D. Arasteh, "THERM 2.0: Program Description," LBNL Report 37371 Rev. 2, Berkeley, CA, 1998.
5. H.F. Sullivan, J.L. Wright, and R.A. Fraser, "Overview of a Project to Determine the Surface Temperatures of Insulated Glazing Units: Thermographic Measurements and 2-D Simulation." ASHRAE Transactions 102(2), American Society of Heating, Refrigerating and Air-Conditioning Engineers Inc., Atlanta GA, 1996.
6. H. Elmahdy, "Surface Temperature Measurement of Insulated Glass Units Using Infrared Thermography." ASHRAE Transactions 102(2), American Society of Heating, Refrigerating and Air-Conditioning Engineers Inc., Atlanta GA, 1996.

7. B.T. Griffith, D. Türler, and D. Arasteh, "Surface Temperatures of Insulated Glazing Units: Infrared Thermography Laboratory Measurements." ASHRAE Transactions 102(2), American Society of Heating, Refrigerating and Air-Conditioning Engineers Inc., Atlanta GA, 1996.

Ernest Orlando Lawrence Berkeley National Laboratory
One Cyclotron Road | Berkeley, California 94720

Prepared for the U.S. Department of Energy under Contract No. DE-AC03-76SF00098